Frequency Domain Functional Near-Infrared Spectrometer (fNIRS) for Crew State Monitoring

Jeffrey R. Mackey and Richard T. Powis
Vantage Partners, LLC, Brook Park, Ohio

Joanne C. Walton, Kristen M. Hauser, and Charles S. Hall
Glenn Research Center, Cleveland, Ohio

Daniel J. Gotti
Universities Space Research Association, Glenn Research Center, Cleveland, Ohio

Angela R. Harrivel
Langley Research Center, Hampton, Virginia

NASA STI Program . . . in Profile

Since its founding, NASA has been dedicated to the advancement of aeronautics and space science. The NASA Scientific and Technical Information (STI) Program plays a key part in helping NASA maintain this important role.

The NASA STI Program operates under the auspices of the Agency Chief Information Officer. It collects, organizes, provides for archiving, and disseminates NASA's STI. The NASA STI Program provides access to the NASA Technical Report Server—Registered (NTRS Reg) and NASA Technical Report Server—Public (NTRS) thus providing one of the largest collections of aeronautical and space science STI in the world. Results are published in both non-NASA channels and by NASA in the NASA STI Report Series, which includes the following report types:

- TECHNICAL PUBLICATION. Reports of completed research or a major significant phase of research that present the results of NASA programs and include extensive data or theoretical analysis. Includes compilations of significant scientific and technical data and information deemed to be of continuing reference value. NASA counter-part of peer-reviewed formal professional papers, but has less stringent limitations on manuscript length and extent of graphic presentations.

- TECHNICAL MEMORANDUM. Scientific and technical findings that are preliminary or of specialized interest, e.g., "quick-release" reports, working papers, and bibliographies that contain minimal annotation. Does not contain extensive analysis.

- CONTRACTOR REPORT. Scientific and technical findings by NASA-sponsored contractors and grantees.

- CONFERENCE PUBLICATION. Collected papers from scientific and technical conferences, symposia, seminars, or other meetings sponsored or co-sponsored by NASA.

- SPECIAL PUBLICATION. Scientific, technical, or historical information from NASA programs, projects, and missions, often concerned with subjects having substantial public interest.

- TECHNICAL TRANSLATION. English-language translations of foreign scientific and technical material pertinent to NASA's mission.

For more information about the NASA STI program, see the following:

- Access the NASA STI program home page at http://www.sti.nasa.gov

- E-mail your question to help@sti.nasa.gov

- Fax your question to the NASA STI Information Desk at 757-864-6500

- Telephone the NASA STI Information Desk at 757-864-9658

- Write to:
  NASA STI Program
  Mail Stop 148
  NASA Langley Research Center
  Hampton, VA 23681-2199
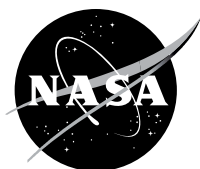
Frequency Domain Functional Near-Infrared Spectrometer (fNIRS) for Crew State Monitoring

Jeffrey R. Mackey and Richard T. Powis
Vantage Partners, LLC, Brook Park, Ohio

Joanne C. Walton, Kristen M. Hauser, and Charles S. Hall
Glenn Research Center, Cleveland, Ohio

Daniel J. Gotti
Universities Space Research Association, Glenn Research Center, Cleveland, Ohio

Angela R. Harrivel
Langley Research Center, Hampton, Virginia

Acknowledgments

Level of Review: This material has been technically reviewed by technical management.

Available from

NASA STI Program
Mail Stop 148
NASA Langley Research Center
Hampton, VA 23681-2199

National Technical Information Service
5285 Port Royal Road
Springfield, VA 22161
703-605-6000

This report is available in electronic form at http://www.sti.nasa.gov/ and http://ntrs.nasa.gov/

Frequency Domain Functional Near-Infrared Spectrometer (fNIRS) for Crew State Monitoring

Jeffrey R. Mackey and Richard T. Powis
Vantage Partners, LLC
Brook Park, Ohio 44142

Joanne C. Walton, Kristen M. Hauser, and Charles S. Hall
National Aeronautics and Space Administration
Glenn Research Center
Cleveland, Ohio 44135

Daniel J. Gotti
Universities Space Research Association
Glenn Research Center
Cleveland, Ohio 44135

Angela R. Harrivel
National Aeronautics and Space Administration
Langley Research Center
Hampton, Virginia 23681

Summary

A frequency domain functional near-infrared spectrometer (fNIRS) and accompanying software have been developed by the NASA Glenn Research Center as part of the Airspace Operations and Safety Program (AOSP) Technologies for Airplane State Awareness (TASA)—SE211 Crew State Monitoring (CSM) Project. The goal of CSM was to develop a suite of instruments to measure the cognitive state of operators while performing operational activities. The fNIRS was one of the instruments intended for the CSM, developed to measure changes in oxygen levels in the brain noninvasively.

Introduction

A frequency domain functional near-infrared spectrometer (fNIRS) and accompanying software have been developed by the NASA Glenn Research Center as part of the Airspace Operations and Safety Program (AOSP) Technologies for Airplane State Awareness (TASA)—SE211 Crew State Monitoring (CSM) Project. The goal of CSM was to develop a suite of instruments to measure the cognitive state of operators while performing operational activities. The fNIRS was one of the instruments intended for the CSM, developed to measure changes in oxygen levels in the brain noninvasively. Ongoing cognitive studies using fNIRS have shown promise that this technology can be used to monitor brain activity by quantifying hemodynamic activations. The fNIRS is a safe, relatively low-cost, nonconfining, and noninvasive technique, implemented by photon scattering a coherent source as it travels through brain tissue. The intensity and phase of the signal are modified according to the change of oxygen level in the hemoglobin. The Glenn-developed fNIRS device uses the frequency domain (FD) multidistance method to reduce signal artifacts generated by movement of the headgear due to vibration, g-levels, or other environmental conditions, and to provide better signal-to-noise margins.
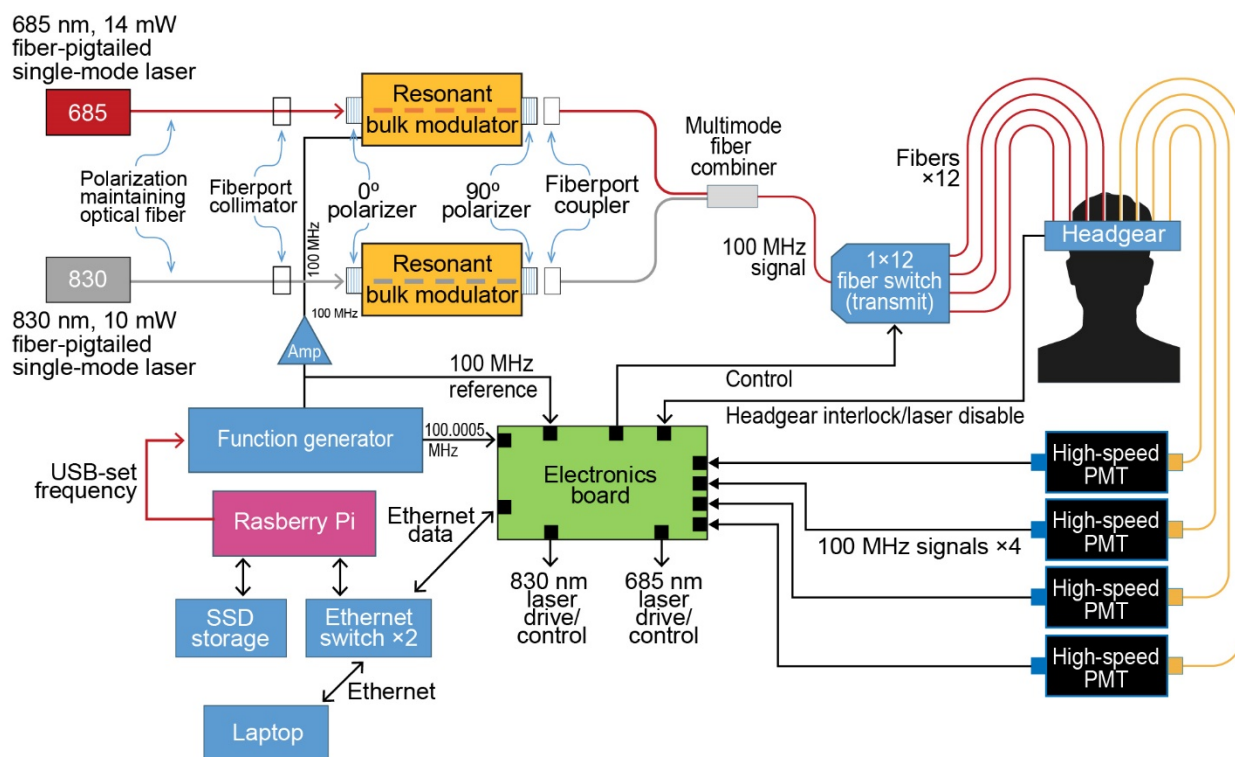
Figure 1.—Functional near-infrared spectrometer (fNIRS) block diagram. Photomultiplier tube is PMT. Solid-state storage device is SSD. Universal serial bus is USB.

A block diagram of the system is shown in Figure 1.

Background Information and System Overview

The overall fNIRS system consists of a FD-based optoelectronic platform, having two discrete-wavelength lasers, an electronic control system, and a data acquisition system. The two lasers are coupled into polarization-maintaining optical fibers and can be modulated at frequencies between 1 Hz and 120 MHz, using the commercial function generator installed in the system. For the final device, modulation frequency was set at 100 MHz with a cross-correlation frequency of 500 Hz (Figure 2).

The electronic control and data acquisition system for the fNIRS is implemented on an Atmel® corporation SAM4E–EK development kit. This approach was taken to save time and resources in system development. By leveraging the development board's power distribution, Ethernet communications, and input/output pin configuration, the system's overall development time and costs were greatly reduced. A custom printed circuit board was designed to provide the necessary functions and interfaces with the rest of the fNIRS system. This "daughterboard" mounts directly onto the general-purpose input/output (GPIO) pins of the development board.

The fNIRS control system is responsible for the synchronization and timing of the fiber optic switches and firing of both the 685- and 830-nm lasers. The system also acquires data from the photomultiplier tubes (PMTs) through their associated amplifiers, mixer, and low-pass filters (LPFs). Cross correlation has been implemented in the fNIRS system for increased noise rejection. The 100-MHz received signals are down converted to 500-Hz signals with amplitude proportional to the received signal's amplitude and phase shift equal to the received signal's phase shift. These data are then digitized and formatted into Ethernet packets that are sent to the Raspberry Pi laptop (pi-top) where they are parsed and saved to a solid-state storage device (SSD).
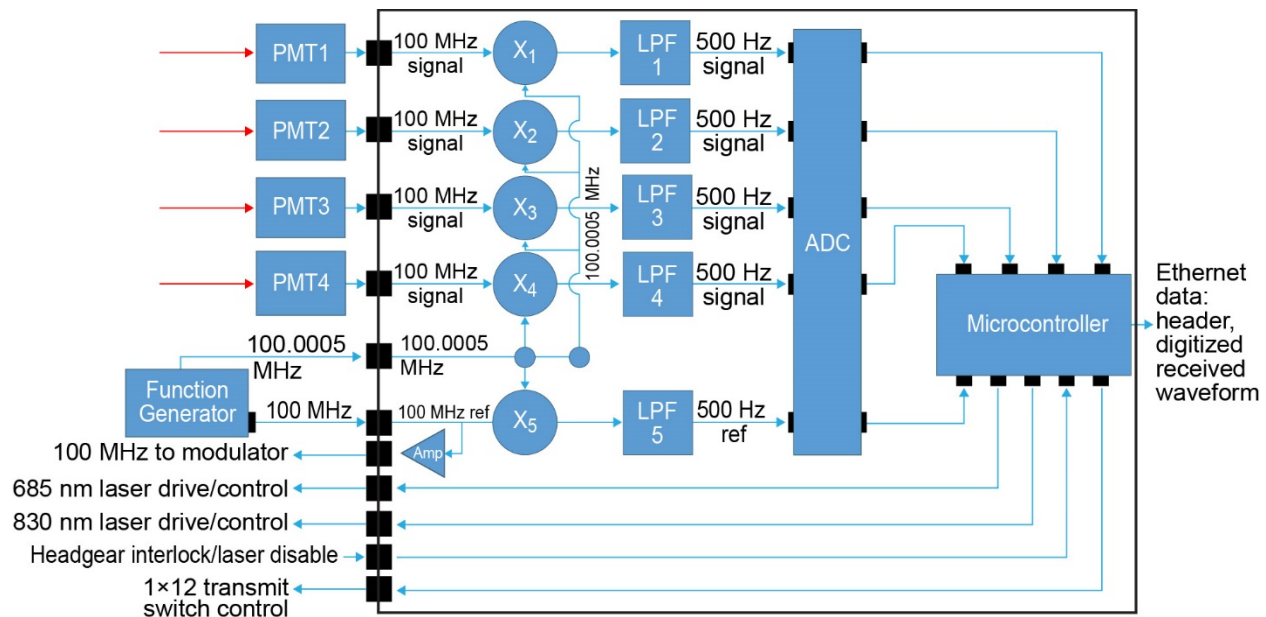
Figure 2.—Functional near-infrared spectrometer (fNIRS) electronics block diagram layout. Analog-to-digital convertor is ADC. Low-pass filter is LPF. Photomultiplier tube is PMT.
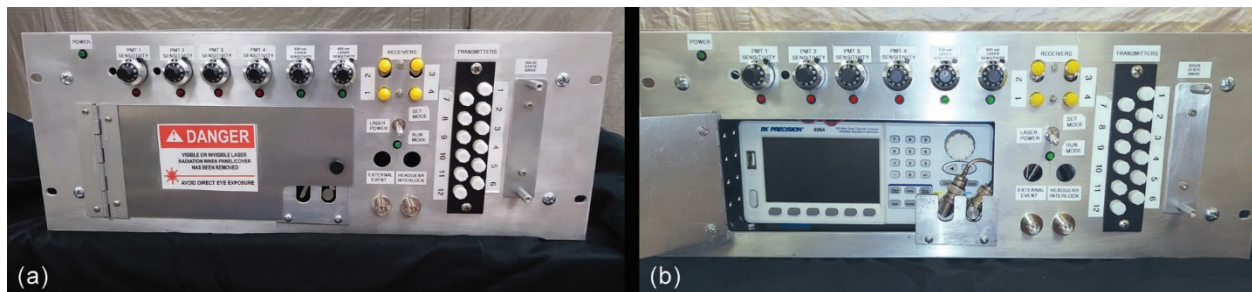

Figure 3.—Functional near-infrared spectrometer (fNIRS) front panel. (a) Front door closed. (b) Front door open.

The fNIRS front panel (Figure 3) allows adjustment of all laser and PMT sensitivities. The internal function generator is accessible to optionally adjust the modulation and cross-correlation frequencies up to system limits; however, the system automatically defaults to 100-MHz modulation and 500-Hz cross-correlation frequencies upon power-up. During normal operation, the front door is closed for shielding against radiofrequency interference. An optional "external event" input is included, which allows the user to mark significant events in the data, either manually using a hand-held button or programmatically via a computer-controlled interface. The SSD can be physically removed from the front panel, but data can also be directly downloaded from the device. Attachments for the headgear also appear on the front panel for easy access.

The fNIRS headgear (Figure 4) consists of a custom flexible headband implementing four optodes configured for the FD multidistance method. Two optodes are located on the forehead (either side of the Fpz position), and two optodes are located near the temples (F4 and F3). Each optode contains three transmitters, spaced linearly 2.5, 3.0, and 3.5 cm apart from one detector. Additional ports are included to allow these distances to be varied. A block between the receiver and the transmitters shields against light scattered from the skin, assuring that only light scattered from deeper structures is received. A safety interlock switch automatically extinguishes the lasers when the headgear is removed. Fiber and electrical attachments to the headgear have been set at a 30 ft length to enable placement of the fNIRS chassis either inside the test location or up to 30 ft away.
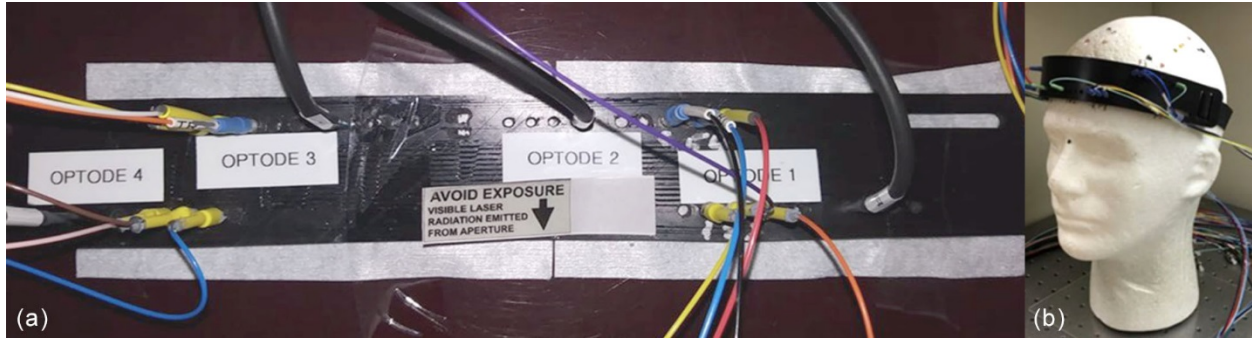
Figure 4.—Functional near-infrared spectrometer (fNIRS) headgear. (a) Headgear. (b) Headgear on model.

Control and data acquisition can be accomplished using either a Raspberry Pi laptop or a personal computer (PC). The pi-top Command Line Toolset is mainly used in troubleshooting. The PC-based CSM Data Analysis Software incorporates control and data acquisition functions with data analysis to calculate absolute changes in oxygenated and deoxygenated hemoglobin concentrations in an easy-to-use graphical user interface (GUI).

The control function of the CSM Data Analysis Software allows the user to start and stop data collection, reset counters, and copy files from the internal SSD to the control computer for faster processing. The analysis function takes the raw signal waveforms (signal and reference) and performs a Fast Fourier Transform (FFT) to calculate alternating current (AC), direct current (DC), phase, and frequency of the original waveform. Scattering, (Eq. (1)), and absorption, (Eq. (2)), coefficients are then calculated from these values. In these equations, all S variables represent the slope of linearization of the attribute with respect to distance, ω is the angular modulation frequency (rad·Hz), and v is the speed of light in the tissue (cm/s).

$$\mu_a = \frac{\omega}{2v}\left(\frac{S_{\text{phase}}}{S_{AC}} - \frac{S_{AC}}{S_{\text{phase}}} \right) \tag{1}$$

$$\mu_{s'} = \frac{S_{AC}^2 - S_{\text{phase}}^2}{3\mu_a} - \mu_a \tag{2}$$

These values allow for concentrations of oxygenated (Eq. (3)) and deoxygenated (Eq. (4)) hemoglobin to be calculated. In the following equations, ε is the extinction coefficient, B is the background absorption, and λ is the wavelength of light used.

$$[oxy - Hb] = \frac{\varepsilon_{deoxy-Hb}(\lambda_2)\left[\mu_a(\lambda_1) - B(\lambda_1)\right] - \varepsilon_{deoxy-Hb}(\lambda_1)\left[\mu_a(\lambda_2) - B(\lambda_2)\right]}{\ln(10)\left[\varepsilon_{deoxy-Hb}(\lambda_2)\varepsilon_{oxy-Hb}(\lambda_1) - \varepsilon_{deoxy-Hb}(\lambda_1)\varepsilon_{oxy-Hb}(\lambda_2)\right]} \tag{3}$$

$$[deoxy - Hb] = \frac{\varepsilon_{oxy-Hb}(\lambda_1)\left[\mu_a(\lambda_2) - B(\lambda_2)\right] - \varepsilon_{oxy-Hb}(\lambda_2)\left[\mu_a(\lambda_1) - B(\lambda_1)\right]}{\ln(10)\left[\varepsilon_{deoxy-Hb}(\lambda_2)\varepsilon_{oxy-Hb}(\lambda_1) - \varepsilon_{deoxy-Hb}(\lambda_1)\varepsilon_{oxy-Hb}(\lambda_2)\right]} \tag{4}$$

FFT waveforms can be displayed from the GUI (Figure 5); four graphs are available for viewing:

1. Wave: raw data
2. Reference amplitude: FFT results, frequency and amplitude, of the reference wave
3. Signal amplitude: FFT results, frequency and amplitude, of the signal wave
4. Signal phase: FFT results, phase shift, of the signal wave from the reference

Information about the data point is located at the top left corner of the display as well as a selection of data points to view from the data file. Data points can be selected for display from the list box, and the graphs and result information update accordingly.
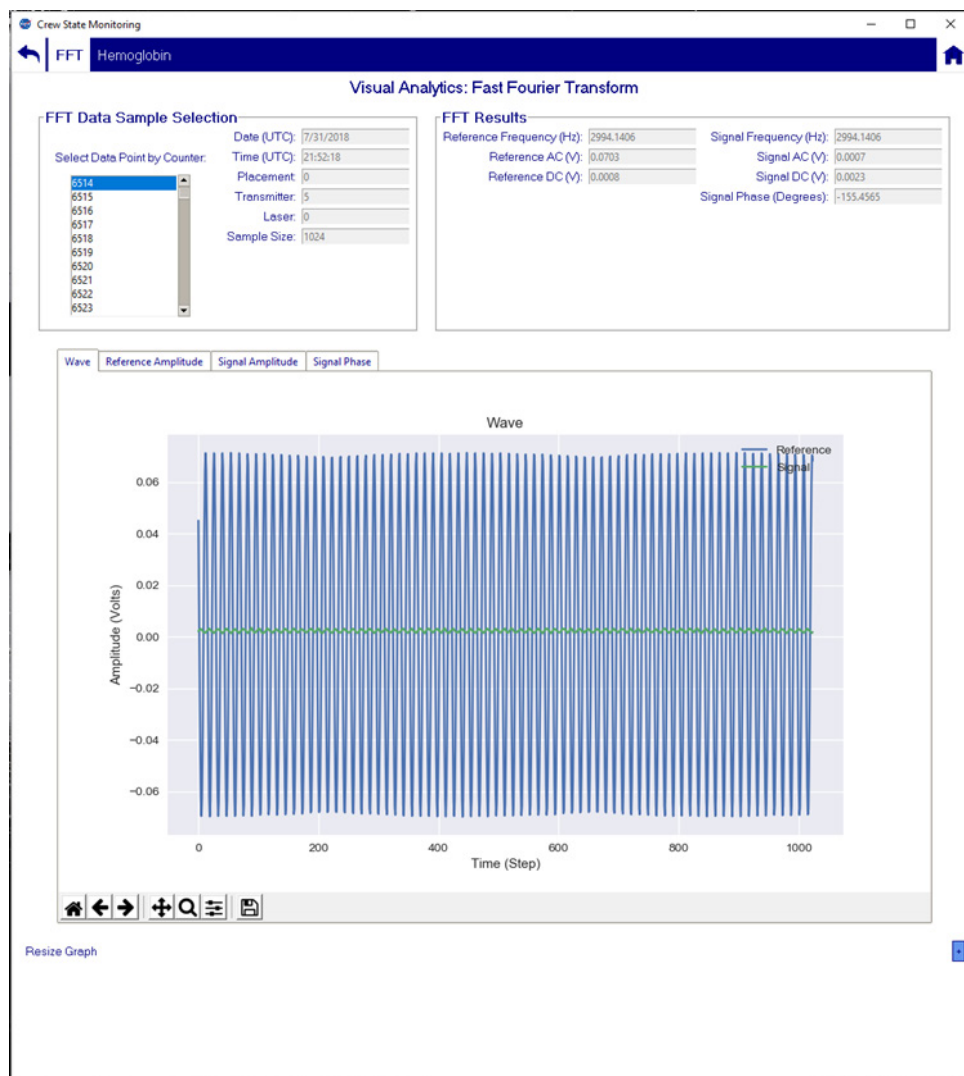

Figure 5.—Fast Fourier Transform (FFT) calculation graphical user interface (GUI) shown with notional test data.

Calculated hemoglobin data for a specified time interval are displayed as shown in Figure 6; four graphs are available for viewing:

1. Absorption coefficients: calculated absorption coefficients for the two waves
2. Scattering coefficients: calculated scattering coefficients for the two waves
3. Hemoglobin concentration: calculated oxygenated and deoxygenated hemoglobin concentrations
4. Percent oxygenated: percent of oxygenated hemoglobin

Hemoglobin is calculated by individual optode, and the graphs update upon selection of a different optode from the list box. The optode name in the list box can be customized by the user.
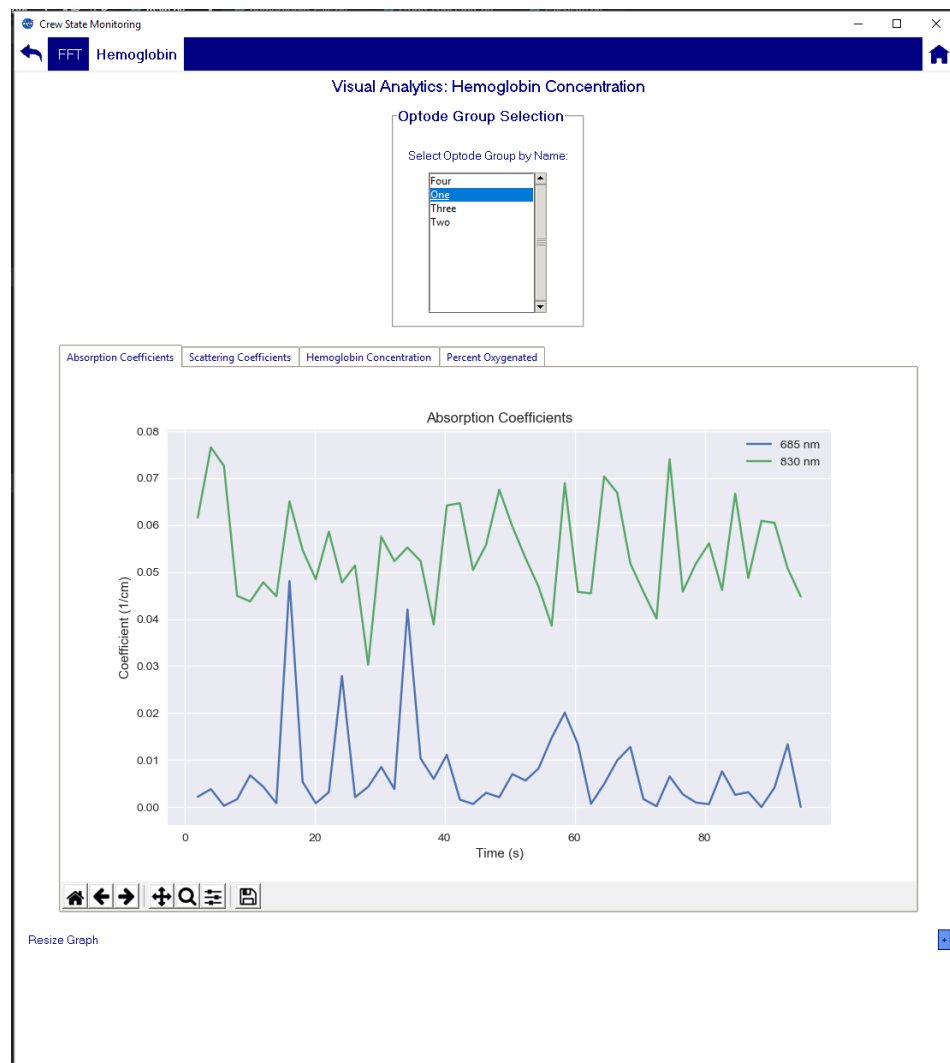

Figure 6.—Oxygenated hemoglobin calculations shown with notional test data.

System Testing and Characterization

Initial functional system characterization was performed by first aligning and characterizing both modulated laser systems coupled to the headgear. The optical system was configured with the two polarizers crossed (polarization axes orthogonal to each other with the modulator aligned and mounted in between the two orthogonal polarizers). For the 685-nm optical input system, two Glan-Thompson (GT) polarizers were used. For the 830-nm optical input system, a GT polarizer was used on the continuous wave input beam, but a special polarizer with a shorter optical path length was used at the output of the electro-optic modulator to preserve modulation amplitude.

Once the optical input systems were aligned and optimized, the function generator output was optimized for the modulated 685-nm laser system. The optical system was characterized using a gray matter phantom manufactured by ISS, Inc. The modulated and switched laser systems were connected to the headgear optodes, and the fiber-coupled amplified PMT voltage outputs were monitored on a 500-MHz digital storage oscilloscope. The PMT signals were recorded at transmitter distances of 2.0, 2.5, 3.0, and 3.5 cm to the fiber-bundle receiver. The modulator driver signal was recorded as the "reference" signal along with a baseline signal with the laser beam blocked. The results from one of the optodes are displayed in Figure 7.

In Figure 7, the AC amplitudes for each transmitter position of the headgear are plotted with respect to the reference signal. Even with zero laser signal (beam blocked) there is a small baseline AC amplitude, but the decrease in signal amplitude and increase in phase shift with increasing transmitter-to-detector spacing is as expected.
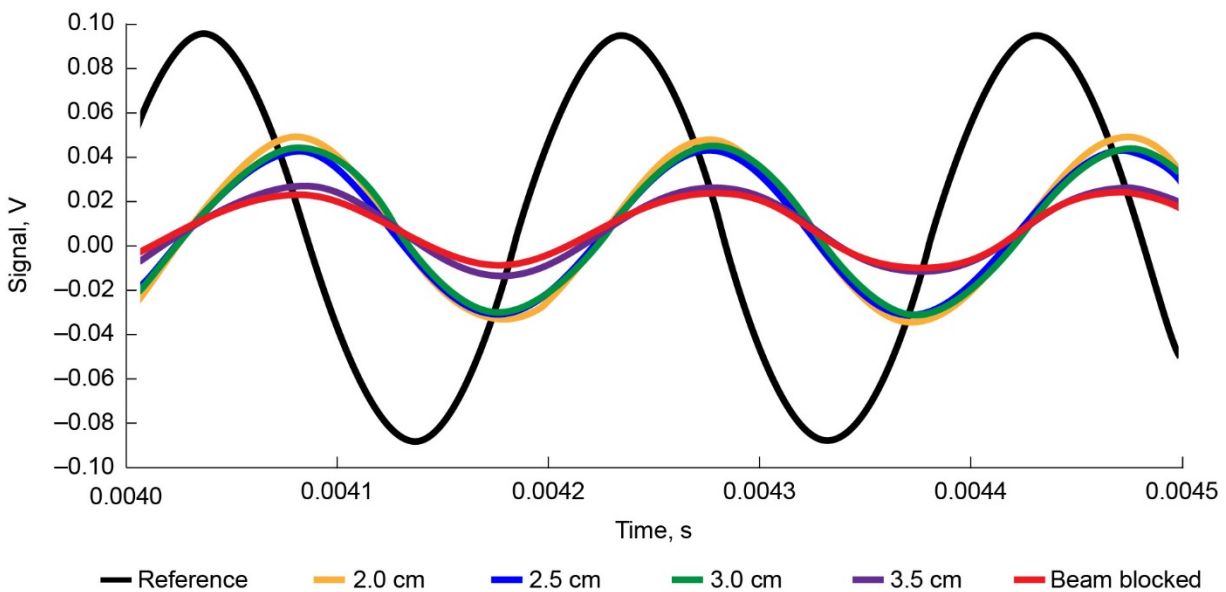

Figure 7.—Gray matter phantom transmitter-to-receiver signals at 2.0, 2.5, 3.0, and 3.5 cm separation.

In order to characterize the electronic control and switching systems in conjunction with the electro-optic modulation system, headgear optodes, and detector electronics, the output signals from the custom mixer-LPF were observed and recorded using the 500-MHz digital storage oscilloscope. Figure 8 illustrates the test configuration. In order to obtain oscilloscope trace data for the signals produced by the headgear and gray matter phantom, the four PMT-amplifier-mixer-LPF signals were directed to the 500-MHz digital storage oscilloscope, bypassing the fNIRS controller, analog-to-digital converter (ADC), and Raspberry Pi.

To characterize the signals received through the receiver bundles into the PMTs, it is important to understand the firing sequence of the fiber optic transmitters on each optode. The transmitters fire in a sequence from greatest to smallest transmitter-to-receiver separation distance. Therefore, an expected observation would be for the signal amplitudes to increase from transmitters 3 to 1. Figure 9 shows the transmitter firing sequence used for all four optodes in the fNIRS instrument.

The transmitter firing sequence is governed by the DiCon Fiberoptics, Inc., 1×12 fiber optic microelectromechanical system (MEMS) switch. The results and limitations of the firing sequence, electronic timing, and available laser power are discussed in the following section.
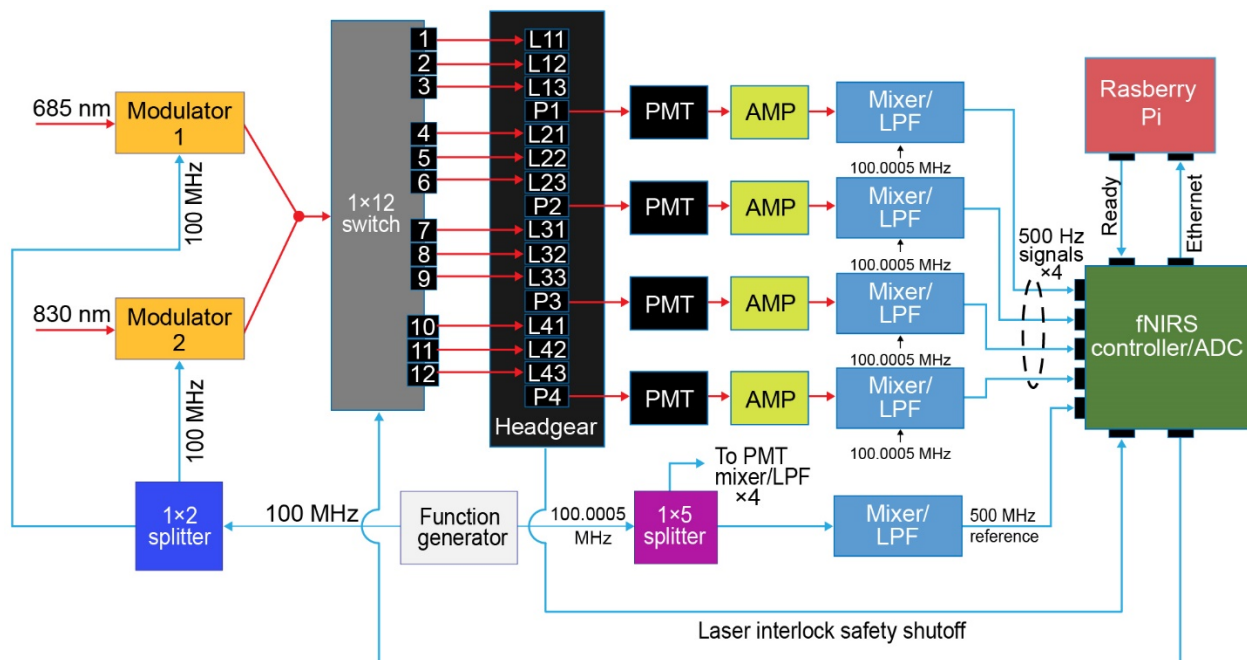

Figure 8.—Test configuration used in switch testing and optoelectronic system characterization. Analog-to-digital convertor is ADC; amplifier, AMP; functional near-infrared spectrometer, fNIRS; low-pass filter, LPF; and photomultiplier tube, PMT.
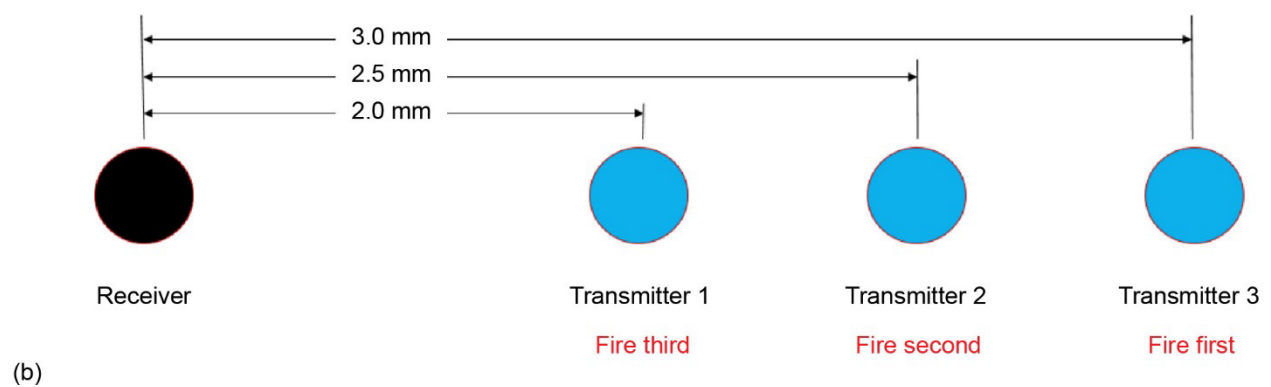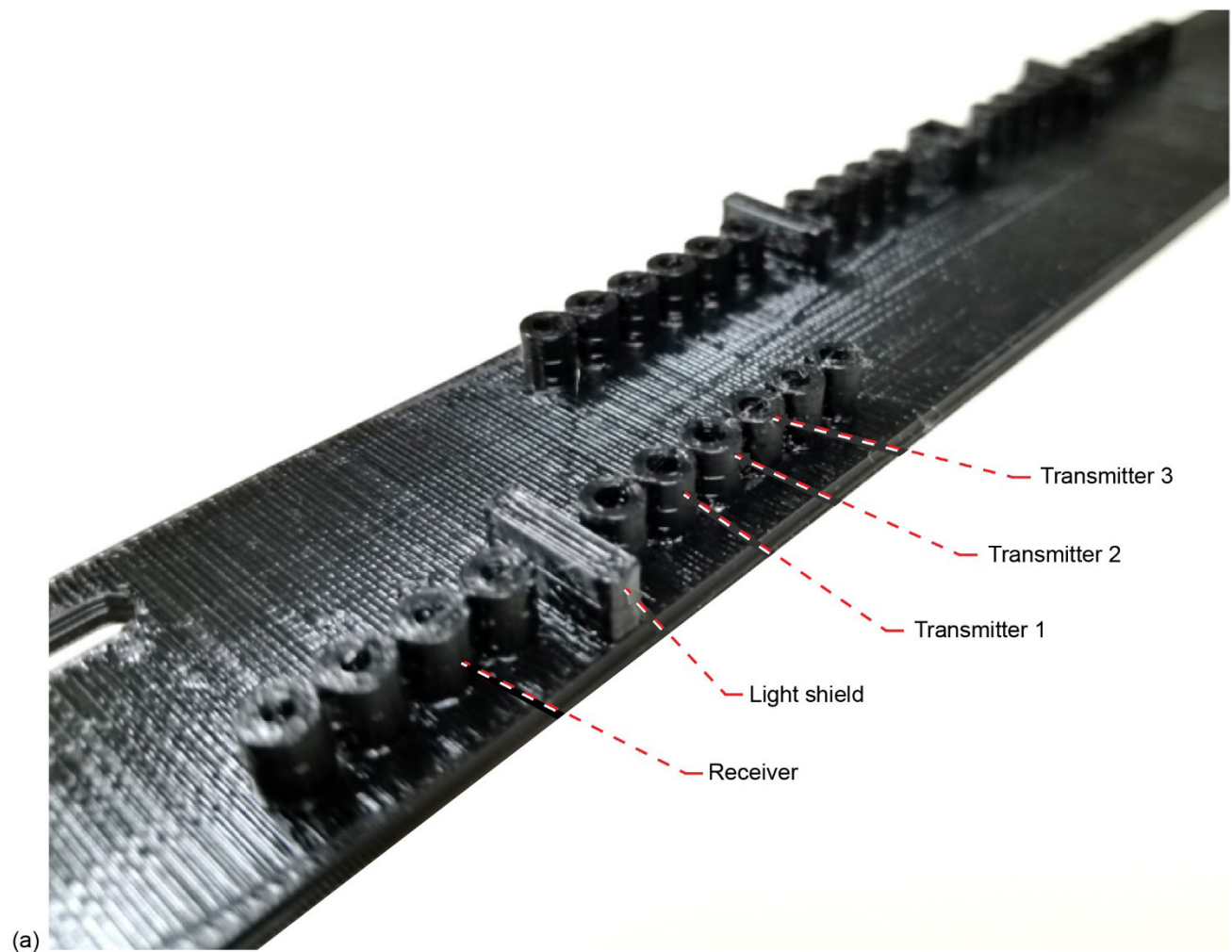
(a)

(b)

Figure 9.—Functional near-infrared spectrometer (fNIRS) three-dimensional-printed headband and transmitter firing sequence.

Results and Discussion

In Figure 10, results obtained for a single optode (consisting of three transmitters and one receiver) indicate the correct firing sequence is implemented; the received signal amplitudes increase as transmitter-to-receiver separation distances decrease. Fiber optic switching time is roughly 5 ms, and the lasers fire for a duration of approximately 50 ms.

Figure 10 also shows that the signal content from optode 1 includes the correct on/off timing pattern along with appropriate switching between the three transmitter fibers. The laser ON time is adjustable, but the time required to switch between each of the 12 transmitters is limited by the DiCon fiber optic switch and cannot be shortened. Transmitter firing times were designed to satisfy a system requirement that measurements on all four optodes occur at a frequency of less than 1 Hz.

Figure 11 shows the signals obtained from all four optodes during normal operation with the headgear placed on a gray matter phantom.

The four signals labeled PMT1, PMT2, PMT3, and PMT4 comprise the PMT-amplifier-mixer-LPF signals that were directed to the 500-MHz digital storage oscilloscope, bypassing the fNIRS controller-ADC and Raspberry Pi. The plots do not include any ADC or postprocessing software artifacts.

From Figure 11, signals were observed from optode 1 on PMT1 (red plot) for transmitter 3 first. The signal on PMT1 from transmitter 3 occurs on the timescale from 0.45 to 0.50 s. The second signal observed occurs on PMT1 from transmitter 2 between 0.50 and 0.55 s. The third signal observed occurs on PMT1 from transmitter 1 between 0.55 and 0.60 s. As expected, all signals increase in amplitude as transmitter-to-receiver distance decreases.

The next set of three transmitters fire in optode 2 on PMT2 (green plot). These signals on PMT2 from transmitter 3 are between 0.60 and 0.65 s, from transmitter 2 are between 0.65 and 0.70 s, and from transmitter 1 are between 0.70 and 0.75 s. Again as expected, all signals increase in amplitude as transmitter-to-receiver distance decreases.
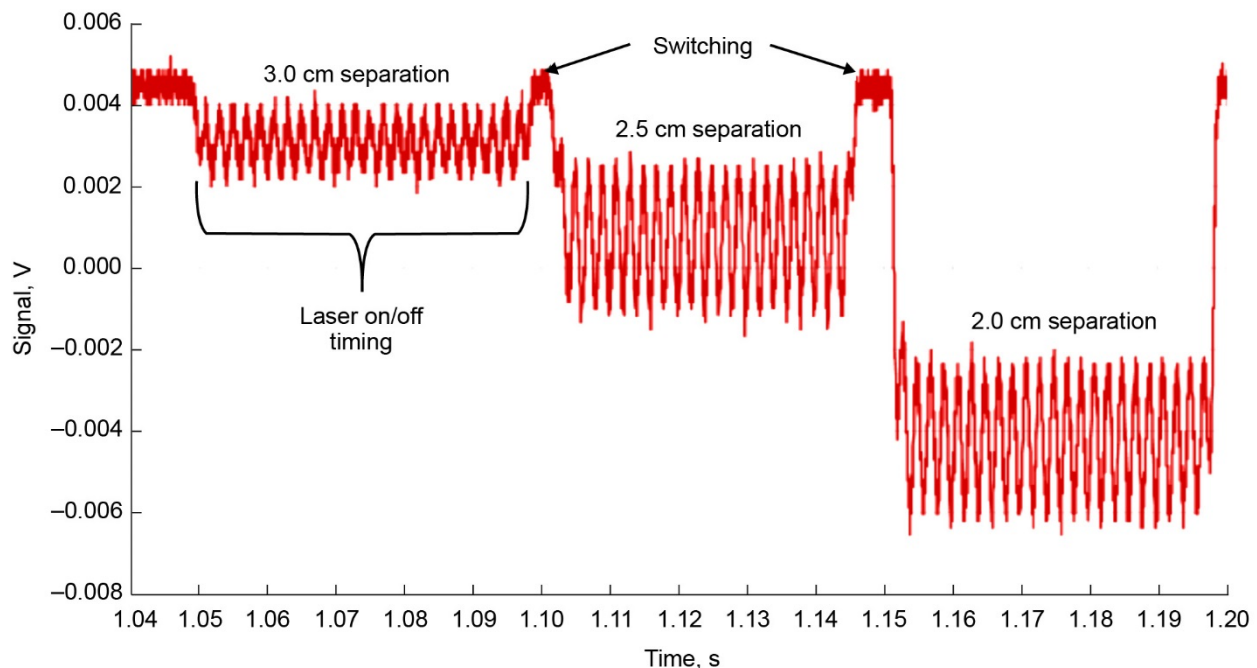

Figure 10.—Single optode received signal obtained from three transmitters in optode 1 firing into a gray matter phantom.
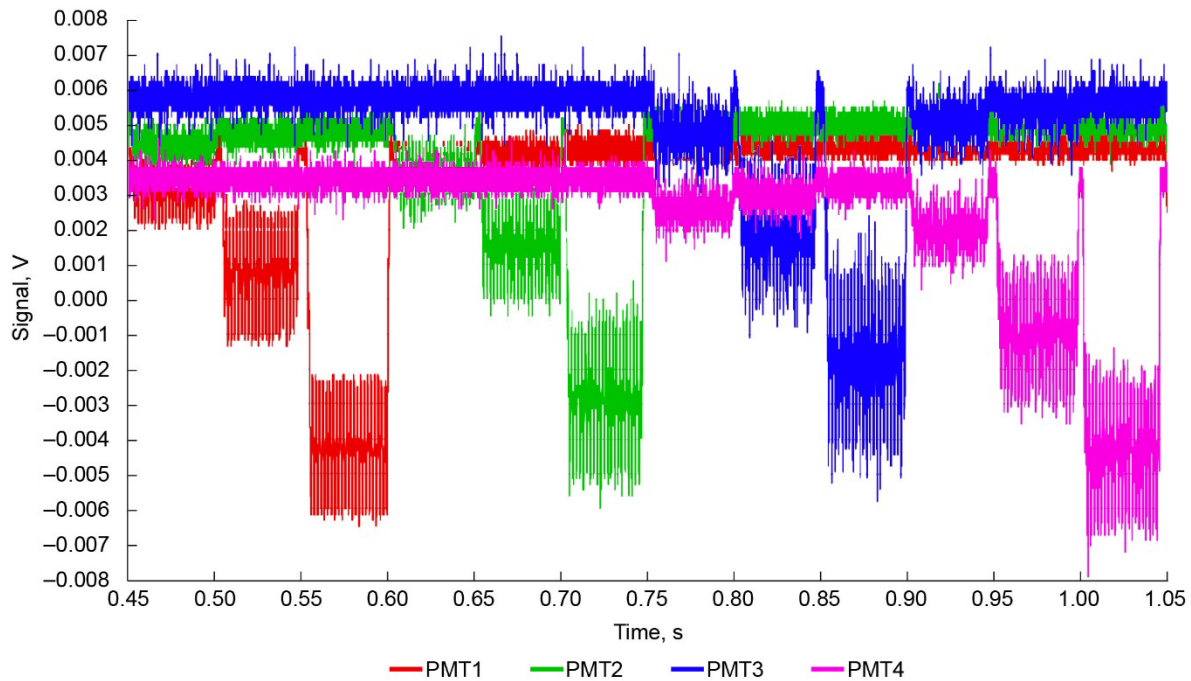
Figure 11.—Signals from all four optodes using digital storage oscilloscope and functional near-infrared spectrometer (fNIRS) headgear mounted on gray matter phantom.

Optode 3 (blue plot) shows signals on PMT3 from transmitter 3 between 0.75 and 0.80 s, from transmitter 2 between 0.80 and 0.85 s, and from transmitter 1 between 0.85 and 0.90 s. Once again, all signals increase in amplitude as transmitter-to-receiver distance decreases.

Optode 4 (purple plot) shows signals on PMT4 from transmitter 3 between 0.90 and 0.95 s, from transmitter 2 between 0.95 and 1.00 s, and from transmitter 1 between 1.00 and 1.05 s. All signals increase in amplitude as transmitter-to-receiver distance decreases.

Some crosstalk is apparent between PMT1 and PMT2 as well as between PMT3 and PMT4. This crosstalk does not require any mitigation because all PMT signals are interrogated only during the time of their primary firing. For example, the crosstalk from PMT4 will be ignored because only signals from PMT3 are recorded between 0.75 and 0.90 s.

The signal data as shown in Figure 11 were recorded to the fNIRS SSD attached to the Raspberry Pi and later analyzed using the CSM Data Analysis Software in order to obtain AC, DC, and phase components. Even though the signals were of similar amplitude from each transmitter-receiver pair in each optode, the software indicated zero values on certain channels that varied per test under the same test conditions. Since the AC, DC, and phase components are digitized using a 24-bit ADC, adequate signal content should be preserved to accommodate the computations.

There are several possibilities concerning the zero values obtained by the software analysis. One is more laser energy may need to be integrated into the signal to aid with the threshold level and provide adequate signal for analysis. Because of the polarization-maintaining fiber optic coupling of the lasers, only 14 and 10 mW are available from the 685- and 830-nm laser fiber outputs, respectively. Both output powers are below the skin maximum permissible exposure (MPE) power limits of 19.2 mW for the 685-nm laser and 35.0 mW for the 830-nm laser as shown in Figure 12.

MPE Calculations for Jeff Mackey – 5/30/17

Skin MPE for fNIRS system

Wavelengths: 685nm and 830nm

Limiting Aperture: 3.5mm -> Area = 9.62*10^-2 cm^2

Exposure Duration 10s > t > 30000s

$$MPE = 0.2\, C_A \left[\frac{W}{cm^2}\right] \quad - \text{ Reference: Pg 87 Table 7b of ANSI Z136.1} - 2014$$

$$C_A = 1.0 \ @685\ nm$$

$$C_A = 10^{0.002*(\lambda-700)} = 1.82\ @830\ nm$$

$$C_A = 1.0 \ @685\ nm$$

$$\varphi \overset{\text{def}}{=} Allowable\ Output\ Power = MPE * Limiting\ Area$$

1) 685 nm

$$MPE = 0.2 * 1.0 \left[\frac{W}{cm^2}\right] = 0.2 \left[\frac{W}{cm^2}\right]$$

$$\varphi = MPE * Limiting\ Area = 0.2 \left[\frac{W}{cm^2}\right] * 9.62 * 10^{-2}[cm^2]$$

$$\varphi = 0.0192\ [W] = 19.2\ [mW]$$

2) 830 nm

$$MPE = 0.2 * 1.82 \left[\frac{W}{cm^2}\right] = 0.364 \left[\frac{W}{cm^2}\right]$$

$$\varphi = MPE * Limiting\ Area = 0.364 \left[\frac{W}{cm^2}\right] * 9.62 * 10^{-2}[cm^2]$$

$$\varphi = 0.035\ [W] = 35\ [mW]$$

Figure 12.—Skin maximum permissible exposure (MPE) limits for functional near-infrared spectrometer (fNIRS) at 685 and 830 nm.

There are two ways to provide more laser energy. One way is to obtain lasers capable of higher power output levels, which might involve different laser driver circuitry. However, the present system is already near the MPE, using the 685-nm laser. The 830-nm laser power could be increased significantly if a suitable laser could be found.

The other method to provide more laser energy would be to increase the integration time greater than 50 ms. Doing so would slow down the full cycle measurement frequency to a value less than 1 Hz, which was a system requirement. If the sampling frequency requirement could be relaxed, integration time will be increased by changing the fiber optic switch timing, allowing signal content to increase.

Concluding Remarks

Based on the results obtained from the photomultiplier tube (PMT)-mixer-low-pass filter signals from the headgear on a gray matter phantom, the optical and electronics systems produce signals of adequate amplitude for frequency domain interrogation on a gray matter phantom. There is some optical crosstalk between neighboring optodes (PMT1 and PMT2 as well as PMT3 and PMT4), but such crosstalk is ignored during signal analysis because of the timing mandated by the electronic control systems. The fiber optic switching, laser timing, modulation, and cross correlation all function properly.

One possibility concerning the zero values obtained by the software analysis is the laser power limitation of the current system. More laser energy integrated into the signal may aid the threshold level and provide adequate signal for analysis. This can be accomplished by using a higher power output laser or increasing integration time. Further signal analysis software refinement is also recommended since it is

unknown why signals of similar amplitude and content are successfully analyzed to produce alternating current (AC), direct current (DC), and phase measurements on certain optodes and not on others.

Finally, setting up an Institutional Review Board (IRB) at NASA Glenn Research Center is recommended in order to test the frequency domain functional near-infrared spectrometer (fNIRS) instrumentation on humans while in development and/or improvement phases. Testing on phantom materials does not provide enough information to assure adequate functionality on humans. Using the IRB established at the NASA Langley Research Center requires system development based solely on gray matter phantom information and feedback from Langley on human tests. Such a configuration may work, but is inefficient during the development phase of the instrumentation.